QCD and models on multiplicities in e^+e^- and $p\bar{p}$ interactions

I.M. Dremin[1]

Lebedev Physical Institute, Moscow

Abstract

A brief survey of theoretical approaches to description of multiplicity distributions in high energy processes is given. It is argued that the multicomponent nature of these processes leads to some peculiar characteristics observed experimentally. Predictions for LHC energies are presented. It is shown that similarity of the energy dependence of average multiplicities in different reactions is not enough alone to suggest the universal mechanism of particle production in strongly-interacting systems. Other characteristics of multiplicity distributions depend on the nature of colliding partners.

1 Introduction.

Multiplicity distributions are the most general characteristics of any high energy process of multiparticle production. They depend on the nature of colliding particles and on their energy. Nevertheless, it has been found that their shapes possess some common qualitative features in all reactions studied. At comparatively low energies, these distributions are relatively narrow and have sub-Poissonian shapes. With energy increase, they widen and fit the Poisson distribution. At even higher energies, the shapes become super-Poissonian, i.e. their widths are larger than for Poisson distribution. The width increases with energy and, moreover, some shoulder-like substructures appear.

Their origin is usually ascribed to multicomponent contents of the process. In QCD description of e^+e^--processes these could be subjets formed inside quark and gluon jets (for the reviews see, e.g., [1, 2]). In phenomenological approaches, the multiplicity distribution in a single subjet is sometimes approximated by the negative binomial distribution (NBD) first proposed for hadronic reactions in [3]. For hadron-initiated processes, these peculiarities are often ascribed to multiple parton-parton collisions [4, 5, 6, 7, 8], which could lead, e.g., to two-, three-... ladder formation of the dual parton (DPM) [9] or quark-gluon string (QGSM) [10, 11, 12] models, and/or to different (soft, hard) types of interactions [13, 14]. They become increasingly important as collision energy is increased. These subprocesses are related to the matter state during the collision (e.g., there are speculations about nonhomogeneous matter distribution in impact parameters [15], not to speak of quark-gluon plasma [16] behaving as a liquid [17] etc).

Theoretical description of the subprocesses differs drastically in e^+e^- and $p\bar{p}$ processes. Jet evolution in e^+e^- is well described by the perturbative QCD equations with the only adjustable parameter Λ_{QCD}. This parameter is approximately known from other characteristics and is, therefore, bounded. The production of perturbative gluons and quark-antiquark pairs can be described in terms of dipole or "antenna" radiation. Color interference plays a crucial role. Many predictions of the perturbative QCD approach have been confirmed by experimental data. What concerns multiplicity distributions, their shape in e^+e^- processes is known only implicitly from studies of their moments. This is determined by the fact that the QCD evolution equations are formulated in terms of the generating function. They can be rewritten as equations for the

[1]E-mail: dremin@lpi.ru

moments but not directly for probabilities of n parton emission. Their solutions up to higher order perturbative QCD [18] have predicted some completely new features of the moments. The moments contain also complete information about the distribution. However, the reconstruction of the shape of the distribution from them is not a trivial task. Some attempts to solve the inverse problem [19, 20] and get directly the shape of the multiplicity distribution were successful only in the lowest order perturbative QCD approximations with several additional assumptions.

The situation with hadronic processes is, in some respect, more complicated. The confinement property is essential, and perturbative QCD methods can not be directly applied. Therefore, some models have been developed. Hadron interactions used to be considered as proceeding via collisions of their constituent partons. In pre-parton times, their role was played by pions, and one-meson exchange model [21] dominated. Pions were treated as hadron constituents. Their high energy interaction produced a ladder of one-pion t-channel exchanges with blobs of low energy pion-pion interactions. This is the content of the multiperipheral model. These blobs were first interpreted as ρ-mesons [22] and later called fireballs [23], clusters [24] or clans [25] when higher mass objects were considered. Multiperipheral dynamics tells us that the number of these blobs is distributed according to the Poisson law. It was argued that its convolution with the distribution of the number of pions produced in each center can lead to the negative binomial distribution (NBD) of created particles. This supposition fits experimental data on multiplicity distributions of pp and $p\bar{p}$ reactions at tens of GeV quite well. However, at higher energies this fit by a single NBD becomes unsatisfactory. A shoulder appears at high multiplicities. Sums of NBD with different parameters were used [14] to get agreement with experiment. Better fits are achieved at the expense of a larger number of adjustable parameters. These shortcomings can be minimized if one assumes that each high energy binary parton collision is independent of some others simultaneously proceeding. With this supposition, the whole process is described as a set of independent pair parton interactions (IPPI-model, proposed in [26]). Effective energy of a pair of partons does not depend on how many other pairs interact and what are these interacting partons (quarks or gluons). The number of adjustable parameters does not increase compared to a single NBD if the probabilities of j pairs interactions and the number of active pairs are known.

Earlier, a somewhat different way to account for multiple parton collisions, which generalized the multiperipheral one-ladder model in the framework of the eikonal approximation, was proposed in DPM and QGSM (the latter one takes into account the reggeization of exchanged particles). They differ from IPPI by probabilities of processes with different number of active parton pairs and by multiplicity distributions of final particles. Also, the Lund model [27] with its parton cascades and the string hadronization due to linear increasing QCD potential has been extremely successful in describing many features of multiparticle production. Several Monte Carlo programs implement this model to provide some hints to experimentalists at present day experiments and give predictions at even higher energies (like PYTHIA, FRITIOF etc.). Some assumptions have to be used for the hadronization of partons at the final stage (e.g., these assumptions differ in PYTHIA and HERWIG cluster model). More important, the predictions at higher energies (in particular, for multiplicity distributions) also differ in these models, and it is necessary to try various approaches and confront them to experiment when LHC enters the operation.

2 Moments of multiplicity distributions.

The shape of multiplicity distributions is so complicated that it is difficult to get any analytical expression for it from the solution of QCD equations. It has been obtained only in the simplest perturbative approximations [19, 20]. In particular, it has been demonstrated [20] that the recoil has a profound effect on the multiplicity distribution in QCD jets. It becomes much narrower than according to the leading perturbative term, where energy conservation is not taken into account. However, no shoulders appear. On the contrary, the tail of the distribution is stronger suppressed.

The alternative and, in some sense, more accurate approach is proposed by studies of moments of the distribution. One can get some QCD predictions for these moments [18] up to the higher order of the perturbative expansion. The moments of various ranks contain complete information about multiplicity distributions. Hence, the shape and energy evolution of multiplicity distributions can be quantitatively described by the rank dependence and energy behavior of their moments. Moment analysis of multiplicity distributions can be also performed for the models of hadronic processes as well as for experimental data. Therefore, this approach is common for all processes and methods of analysis.

To introduce moments on most general grounds, we write the generating function $G(E,z)$ of the multiplicity distribution $P(n,E)$

$$G(E,z) = \sum_{n=0}^{\infty} P(n,E)(1+z)^n. \tag{1}$$

The multiplicity distribution is obtained from the generating function as

$$P(n) = \frac{1}{n!}\frac{d^nG(E,z)}{dz^n}\Big|_{z=-1}. \tag{2}$$

In what follows, we will use the so-called unnormalized factorial $\mathcal{F}_q$ and cumulant $\mathcal{K}_q$ moments defined according to the formulas

$$\mathcal{F}_q = \sum_n P(n)n(n-1)...(n-q+1) = \frac{d^qG(E,z)}{dz^q}\Big|_{z=0}, \tag{3}$$

$$\mathcal{K}_q = \frac{d^q \ln G(E,z)}{dz^q}\Big|_{z=0}. \tag{4}$$

They determine correspondingly the total and genuine, i.e., irreducible to lower order correlations among the particles produced (for more details see [28, 2]). First factorial moment defines the average multiplicity $\mathcal{F}_1 = \langle n \rangle$, second one is related to the width (dispersion) of the multiplicity distribution $\mathcal{F}_2 = \langle n(n-1)\rangle$, etc. Factorial and cumulant moments are not independent. They are related by the formula

$$\mathcal{F}_q = \sum_{m=0}^{q-1} C_{q-1}^m \mathcal{K}_{q-m}\mathcal{F}_m, \tag{5}$$

where

$$C_{q-1}^m = \frac{(q-1)!}{m!(q-m-1)!} \tag{6}$$

are the binomial coefficients.

Since both $\mathcal{F}_q$ and $\mathcal{K}_q$ strongly increase with their rank and energy, the ratio

$$H_q = \mathcal{K}_q/\mathcal{F}_q, \tag{7}$$

first introduced in [18], is especially useful due to partial cancellation of these dependences. More important is that some valuable predictions about its behavior can be obtained in perturbative QCD. Also, it will be shown below that H_q moments of the IPPI-model depend on smaller number of its adjustable parameters than factorial and cumulant moments. Thus, even though $\mathcal{F}_q$, $\mathcal{K}_q$ and H_q are interrelated, they can provide knowledge about different facets of the same multiplicity distribution.

It is easy to find the ratio H_q from iterative formulas

$$H_q = 1 - \sum_{p=1}^{q-1} \frac{\Gamma(q)}{\Gamma(p+1)\Gamma(q-p)} H_{q-p} \frac{\mathcal{F}_p \mathcal{F}_{q-p}}{\mathcal{F}_q}, \tag{8}$$

once the factorial moments have been evaluated.

The factorial moments $\mathcal{F}_q$'s are always positive by definition (Eq. (3)). The cumulant moments $\mathcal{K}_q$'s can change sign. They are equal to 0 for Poisson distribution. Consequently, $H_q = 0$ in this case.

Let us emphasize that H_q moments are very sensitive to minute details of multiplicity distributions and can be used to distinguish between different models and experimental data.

3 QCD on moments in e^+e^- collisions.

All moments can be calculated from the generating function as explained above. The generating functions for quark and gluon jets satisfy definite equations in perturbative QCD (see [19, 2]). They are

$$\begin{aligned} G'_G &= \int_0^1 dx K_G^G(x)\gamma_0^2[G_G(y+\ln x)G_G(y+\ln(1-x)) - G_G(y)] \\ &+ n_f \int_0^1 dx K_G^F(x)\gamma_0^2[G_F(y+\ln x)G_F(y+\ln(1-x)) - G_G(y)], \end{aligned} \tag{9}$$

$$G'_F = \int_0^1 dx K_F^G(x)\gamma_0^2[G_G(y+\ln x)G_F(y+\ln(1-x)) - G_F(y)], \tag{10}$$

where the labels G and F correspond to gluons and quarks, the energy scale of the process is defined by $y = \ln Q/Q_0$, $Q = p\Theta$ is a virtuality of a jet, $p \approx \sqrt{s}/2$ is its momentum, Θ opening angle, Q_0=const. Here $G'(y) = dG/dy$, n_f is the number of active flavors,

$$\gamma_0^2 = \frac{2N_c\alpha_S}{\pi}. \tag{11}$$

The running coupling constant in the two-loop approximation is

$$\alpha_S(y) = \frac{2\pi}{\beta_0 y}\left(1 - \frac{\beta_1}{\beta_0^2}\cdot\frac{\ln 2y}{y}\right) + O(y^{-3}), \tag{12}$$

where

$$\beta_0 = \frac{11N_c - 2n_f}{3}, \qquad \beta_1 = \frac{17N_c^2 - n_f(5N_c + 3C_F)}{3}. \tag{13}$$

The kernels of the equations are

$$K_G^G(x) = \frac{1}{x} - (1-x)[2 - x(1-x)], \tag{14}$$

$$K_G^F(x) = \frac{1}{4N_c}[x^2 + (1-x)^2], \tag{15}$$

$$K_F^G(x) = \frac{C_F}{N_c}\left[\frac{1}{x} - 1 + \frac{x}{2}\right], \tag{16}$$

N_c=3 is the number of colors, and $C_F = (N_c^2 - 1)/2N_c = 4/3$ in QCD.

Herefrom, one can get equations for any moment of the multiplicity distribution both for quark and gluon jets. One should just equate the terms with the same powers of $u = 1 + z$ in both sides of the equations where expressions (1) are substituted for both quarks and gluons.

In particular, the non-trivial energy dependence of mean multiplicity in quark and gluon jets has been predicted. Within two lowest perturbative QCD approximations it has a common behavior

$$\langle n_{G,F}\rangle = A_{G,F}\, y^{-a_1 c^2} \exp(2c\sqrt{y}), \tag{17}$$

where $A_{G,F}$=const, $c = (4N_c/\beta_0)^{1/2}$, $a_1 \approx 0.3$.

Main features of the solutions can be demonstrated in gluodynamics where only first equation with $n_f = 0$ is considered. At asymptotically high energies it can be reduced [19] to the differential equation

$$[\ln G(y)]'' = \gamma_0^2[G(y) - 1]. \tag{18}$$

From the moments definitions, one can easily guess that this equation determines the asymptotic behavior of H_q because $\ln G$ in the left-hand side gives rise to $\mathcal{K}_q$ and G in the right-hand side to $\mathcal{F}_q$. The second derivative in the left-hand side would result in the factor q^2. Thus, it can be shown [18] that asymptotical ($y \to \infty$) values of H_q moments are positive and decrease as q^{-2}. At present energies they become negative at some values of q and reveal the negative minimum at

$$q_{min} = \frac{1}{h_1\gamma_0} + 0.5 + O(\gamma_0), \tag{19}$$

where $h_1 = b/8N_c = 11/24$, $b = 11N_c/3 - 2n_f/3$. At Z^0 energy $\alpha_S \approx 0.12$, and this minimum is located at about $q \approx 5$. It moves to higher ranks with energy increase because the coupling strength decreases. Some hints to possible oscillations of H_q vs q at higher ranks at LEP energies were obtained in [18]. They were obtained with account of recoil effects in the higher order perturbative QCD and stressed the importance of energy conservation in high energy processes so often mentioned by Bo Andersson (see [27]). The approximate solution of the gluodynamics equation for the generating function [29] agrees with this conclusion and predicts the oscillating behavior at higher ranks. The same conclusions were obtained from exact solution of equations for quark and gluon jets in the framework of fixed coupling QCD [30]. A recent exact numerical solution of the gluodynamics equation in a wide energy interval [31] coincides with the qualitative features of multiplicity distributions described above. These oscillations were confirmed by experimental data for e^+e^- collisions and found also for hadron-initiated processes first in [32], later in [33] and most recently in [34]. This will be demonstrated below in Fig. 10.

However, one should be warned that the amplitudes of oscillations strongly depend on a multiplicity distribution cut-off due to limited experimental statistics (or by another reasoning) if

it is done at rather low multiplicities [35]. Usually there are no such cut-offs in analytical expressions for H_q. One can control the influence of cut-offs by shifting them appropriately. The qualitative features of H_q behavior persist nevertheless. In what follows, we consider very high energy processes where the cut-off due to experimental statistics is practically insignificant. Numerical estimates of the relation between maximum multiplicity measured and effective ranks of the moments is given in Appendix.

4 Negative binomial distribution and IPPI-model.

Independently of progress in perturbative QCD calculations, the NBD-fits of multiplicity distributions were attempted both for e^+e^- and $pp(p\bar{p})$ collisions [14, 36, 37]. The single NBD-parameterization is

$$P_{NBD}(n,E) = \frac{\Gamma(n+k)}{\Gamma(n+1)\Gamma(k)} \left(\frac{m}{k}\right)^n \left(1+\frac{m}{k}\right)^{-n-k}, \tag{20}$$

where Γ denotes the gamma-function. This distribution has two adjustable parameters $m(E)$ and $k(E)$ which depend on energy. However the simple fit by the formula (20) is valid till the shoulders appear. In that case, this formula is often replaced [14] by the hybrid NBD which simply sums up two or more expressions like (20). Each of them has its own parameters m_j, k_j. These distributions are weighted with the energy dependent probability factors w_j which sum up to 1. Correspondingly, the number of adjustable parameters drastically increases if the distributions are completely unrelated.

It was proposed recently [26] that hadron interactions can be represented by a set of Independent Pair Parton Interactions (IPPI-model). This means that colliding hadrons are considered as "clouds" of partons which interact pairwise. It is assumed that each binary parton collision is described by the same NBD distribution. The only justification for this supposition is given by previous fits of multiplicity distributions at lower energies. Then the convolution of these distributions, subject to a condition that the sum of binary collision multiplicities is the total multiplicity n, leads [26] to a common distribution

$$P(n;m,k) = \sum_{j=1}^{j_{max}} w_j P_{NBD}(n; jm, jk). \tag{21}$$

This is the main equation of IPPI-model. One gets a sum of negative binomial distributions with shifted maxima and larger widths for a larger number of collisions. No new adjustable parameters appear in the distribution for j pairs of colliding partons. The probabilities w_j are determined by collision dynamics and, in principle, can be evaluated if some model is adopted (e.g., see [11, 12]). Independence of parton pairs interactions implies that at very high energies w_j is a product of j probabilities w_1 for one pair. Then from the normalization condition

$$\sum_{j=1}^{j_{max}} w_j = \sum_{j=1}^{j_{max}} w_1^j = 1 \tag{22}$$

one can find w_1 if j_{max}, which is determined by the maximum number of parton interactions at a given energy, is known. This is the only new parameter. It depends on energy. Thus

three parameters are sufficient to describe multiplicity distributions at any energy. Moreover, asymptotically $j_{max} \to \infty$ and $w_1 = 0.5$ according to (22).

The factorial moments of the distribution (21) are

$$\mathcal{F}_q = \sum_{j=1}^{j_{max}} w_j \frac{\Gamma(jk+q)}{\Gamma(jk)} \left(\frac{m}{k}\right)^q = f_q(k) \left(\frac{m}{k}\right)^q \tag{23}$$

with

$$f_q(k) = \sum_{j=1}^{j_{max}} w_j \frac{\Gamma(jk+q)}{\Gamma(jk)}. \tag{24}$$

For H_q moments one gets

$$H_q = 1 - \sum_{p=1}^{q-1} \frac{\Gamma(q)}{\Gamma(p+1)\Gamma(q-p)} H_{q-p} \frac{f_p f_{q-p}}{f_q}. \tag{25}$$

Note that according to Eqs (24), (25) H_q are functions of the parameter k only and do not depend on m in IPPI-model. This remarkable property of H_q moments provides an opportunity to fit them by one parameter. It is nontrivial because the oscillating shapes of H_q are quite complicated as shown below.

Once the parameter k is found from fits of H_q, it is possible to get another parameter m rewriting Eq. (23) as follows

$$m = k \left(\frac{\mathcal{F}_q}{f_q(k)}\right)^{1/q}. \tag{26}$$

This formula is a sensitive test for the whole approach because it states that the definite ratio of q-dependent functions to the power $1/q$ becomes q-independent if the model is correct. Moreover, this statement should be valid only for those values of k which are determined from H_q fits. Therefore, it can be considered as a criterion of a proper choice of k and of the model validity, in general. This criterion of constancy of m happens to be extremely sensitive to the choice of k as shown below.

In the paper [12], the energy dependence of the probabilities w_j was estimated according to the multiladder exchange model [11] (its various modifications are known as DPM - Dual Parton Model or QGSM - Quark-Gluon String Model). They are given by the following normalized expressions

$$w_j(\xi_j) = \frac{p_j}{\sum_{j=1}^{j_{max}} p_j} = \frac{1}{jZ_j(\sum_{j=1}^{j_{max}} p_j)} \left(1 - e^{-Z_j} \sum_{i=0}^{j-1} \frac{Z_j^i}{i!}\right) \tag{27}$$

where

$$\xi_j = \ln(s/s_0 j^2), \quad Z_j = \frac{2C\gamma}{R^2 + \alpha'_P \xi_j} \left(\frac{s}{s_0 j^2}\right)^\Delta \tag{28}$$

with numerical parameters obtained from fits of experimental data on total and elastic scattering cross sections: $\gamma = 3.64$ GeV^{-2}, $R^2 = 3.56$ GeV^{-2}, $C = 1.5$, $\Delta = \alpha_P - 1 = 0.08$, $\alpha'_P = 0.25$ GeV^{-2}, s_0 =1 GeV^2. It is seen that each w_j depends on 6 adjustable parameters in these models.

Below, we will use both possibilities (22) and (27) in our attempts to describe experimental data. The probabilities w_j are different for them (see Table 1). In IPPI-model they decrease exponentially with the number of active partons, while in the ladder models they are inverse

proportional to this number with additional suppression at large j due to the term in brackets in (27). This is the result of the modified eikonal approximation. Let us stress that, when we use expressions (27) for probabilities, this does not directly imply comparison with DPM-QGSM because in our case NBD is chosen for the multiplicity distribution in a single ladder, while it is Poisson distribution for resonances in DPM-QGSM. Thus, we will call it the modified ladder model.

We show the values w_j for j_{max}=3 – 6 pairs calculated according to Eq. (22) in the left-hand side of Table 1 and according to Eq. (27) in its right-hand side. These values of j_{max} are chosen because previous analysis of experimental data [8] has shown that 2 pairs become active at energy about 120 GeV and the number of binary collisions increases with energy increasing. Thus, namely these numbers will be used in comparison with experiment at higher energies. In particular, we shall choose j_{max} = 3 at 300 and 546 GeV, 4 at 1000 and 1800 GeV, 5 at 14 TeV and 6 at 100 TeV (see below).

Table 1.

The values of w_j according to (22) (left-hand side) and (27) (right-hand side).

j_{max}	3	4	5	6	3	4	5	6
w_1	0.544	0.519	0.509	0.504	0.562	0.501	0.450	0.410
w_2	0.295	0.269	0.259	0.254	0.278	0.255	0.236	0.219
w_3	0.161	0.140	0.131	0.128	0.160	0.153	0.152	0.147
w_4	0	0.072	0.067	0.065	0	0.091	0.100	0.104
w_5	0	0	0.034	0.033	0	0	0.062	0.073
w_6	0	0	0	0.016	0	0	0	0.047

One can clearly see the difference between the two approaches. The value of w_1 is always larger than 0.5 in the IPPI-model, while it can become less than 0.5 in the (modified) ladder model [9, 11] at high energies. In the ladder model, w_j depend explicitely on energy (not only on j_{max} cut-off). We show their values at 546 and 1800 GeV in the right-hand side columns of j_{max}=3 and 4. Those at 300 and 1000 GeV are larger for w_1 by about 1% and smaller for w_3 by about 3%. When energy increases, the processes with a larger number of active pairs play more important role in the modified ladder approach compared to IPPI-model. Thus, the j_{max} cut-off is also more essential there.

In principle, one can immediately try a two-parameter fit of experimental multiplicity distributions using Eq. (21) if w_j are known according to Eqs. (22) or (27). However, the use of their moments is preferred.

5 Comparison with experiment.

Let us begin with hadronic collisions and then compare them with other processes.

We have compared [26] IPPI-model conclusions with experimental (but extrapolated [8, 38] to the full phase space) multiplicity distributions of E735 [39, 7] collaboration for $p\bar{p}$ collisions at Tevatron energies 300, 546, 1000 and 1800 GeV. The multiplicity of charged particles was divided by 2 to get the multiplicity of particles with the same charge. Then the above formulas for moments were used. Correspondingly, the parameters m and k refer to these distributions.

The parameter j_{max} is chosen according to prescriptions discussed above.

Factorial and H_q moments were obtained from experimental data on $P(n)$ according to Eqs. (3), (8). Experimental H_q moments were fitted by Eq. (25) to get the parameters $k(E)$. We show in Fig. 1 how perfect are these fits at 1.8 TeV for k equal to 3.7 (solid line) and 4.4 (dash-dotted line). At this energy, we considered four active parton pairs with w_j given by Eq. (22). It is surprising that oscillations of H_q moments are well reproduced with one adjustable parameter k. The general tendency of this quite complicated oscillatory dependence is clearly seen.

With these values of the parameter k, we have checked whether m is constant as a function of q as required by Eq. (26). The $m(q)$ dependence is shown in Fig. 2 for the same values of k and for much larger value 7.5. The constancy of m is fulfilled with an accuracy better than 1% for $k = 4.4$ up to $q = 16$. The upper and lower lines in Fig. 2 demonstrate clearly that this condition bounds substantially admissible variations of k.

The same-charge multiplicity distribution at 1.8 TeV has been fitted with parameters $m =$ 12.94 and k=4.4 as shown in Fig. 3 (solid line). To estimate the accuracy of the fit, we calculated $\sum_{n=1}^{125}(P_t(n) - P_e(n))^2/\Delta^2$ over all 125 experimental points. Here, P_t, P_e are theoretical and experimental distributions and Δ is the total experimental error. It includes both statistical and systematical errors. Note that the latter ones are large at low multiplicities in E735 data. This sum is equal to 50 for 125 degrees of freedom. No minimization of it was attempted. This is twice better than the three-parameter fit by the generalized NBD considered in [40]. Poisson distribution of particles in binary collisions is completely excluded. This is shown in Fig. 3 by the dash-dotted line.

The same procedure has been applied to data at energies 300, 546, 1000 GeV. As stated above, we have assumed that 3 binary parton collisions are active at 300 and 546 GeV and 4 at 1000 GeV. We plot in Figs. 5 and 6 the energy dependence of parameters m and k. The parameter m increases with energy logarithmically (Fig. 5). This is expected because increase of $M_1 = \sum w_j j$ due to increasing number of active pairs at these energies leads to somewhat faster than logarithmical increase of average multiplicity in accordance with experimental observations. The energy dependence of k is more complicated and rather irregular (Fig. 6).

We tried to ascribe the latter to the fact that the effective values of k, which we actually find from these fits, depend on the effective number of parton interactions, i.e. on w_j variation at a threshold. The threshold effects can be important in this energy region. Then, the simple relation (22) is invalid. This influences the functions $f_q(k)$ (24) and, consequently, H_q calculated from Eq. (25). One can reduce the effective number of active pairs to about 2.5 at 300 GeV and 3.5 at 1000 GeV if chooses the following values of w_j: 0.59, 0.34, 0.07 at 300 GeV and 0.54, 0.29, 0.14, 0.03 at 1000 TeV instead of those calculated according to (22) and shown in Table 1. This gives rise to values of k which are not drastically different from previous ones. However, the quality of fits becomes worse. Fits with 2 active pairs at 300 GeV and 3 pairs at 1000 GeV fail completely.

Hence, we have to conclude that this effect results from dynamics of hadron interactions which is not understood yet and should be incorporated in the model. The preliminary explanation of this effect could be that at the thresholds of a new pair formation the previous active pairs produce more squeezed multiplicity distributions due to smaller phase-space room available for them because of a newcomer. Therefore, the single pair dispersion would decrease and the k values increase. It would imply that thresholds are marked not only by the change of w_j shown in Table 1 but also by the variation of the parameter k.

The threshold effects become less important at higher energies. We assume that there are 5 active pairs at 14 TeV and 6 at 100 TeV. Then we extrapolate to these energies. The parameter

m becomes equal to 19.2 at 14 TeV and 25.2 at 100 TeV if logarithmical dependence is adopted as shown in Fig. 5 by the straight line. We choose two values of k equal to 4.4 and 8 since we do not know which one is responsible for thresholds. The predicted multiplicity distributions with these parameters are plotted in Fig. 7. The oscillations of H_q still persist at these energies (see Fig. 8). The minima are however shifted to $q = 6$ at 14 TeV and 7 at 100 TeV as expected.

The fit at 1.8 TeV with an approximation of w_j according to the modified ladder model (27) with NBD for a binary parton collision is almost as successful as the fit with values of w_j given by IPPI-model. However, some difference at 14 TeV (see Fig. 7) and especially at 100 TeV between these models is predicted. To keep the same mean multiplicity in both models at the same energy, we have chosen different values of m according to $\langle n \rangle = m \sum w_j j$ and w_j values shown in Table 1. Namely, their ratios are m_{IPPI}/m_{lad} =0.988, 1.039, 1.145, 1.227 for j_{max}=3, 4, 5, 6, correspondingly. This shows that the maximum of the distribution moves to smaller multiplicities and its width becomes larger in the modified ladder model compared to IPPI-model with energy increasing.

Surely, one should not overestimate the success of the IPPI-model in its present initial state. It has been applied just to multiplicity distributions. For more detailed properties, say, rapidity distributions, one would need a model for the corresponding features of the one-pair process. Moreover, the screening effect (often described by the triple Pomeron vertex) will probably become more important at higher energies. All these features are somehow implemented in the well known Monte Carlo programs PYTHIA [42], HERWIG [43] and DPM-QGSM [9, 11] . However, for the latter one, e.g., the multiplicity distribution for a single ladder is given by the Poisson distribution of emission centers (resonances) convoluted with their decay properties, and probabilities w_j contain several adjustable parameters. It differs from the IPPI-model. The latter approach proposes more economic way with a smaller number of such parameters. What concerns the further development of the event generator codes, it is tempting to incorporate there the above approach with a negative binomial distribution of particles created by a single parton pair, and confront the results to a wider set of experimental data. We intend to do it later to learn how it influences other characteristics.

6 Is hadronic production similar in various processes?

This question was first raised by the statement of [41] that the average multiplicities in e^+e^- and $pp(p\bar{p})$ processes increase with energy in a similar way. Recently, PHOBOS Collaboration [44] claimed even that the energy behavior of mean multiplicities in all processes is similar. Therefrom, it has been concluded that the dynamics of all hadronic processes is the same. Beside our general belief in QCD, we can not claim that other characteristics of multiple production processes initiated by different partners coincide. To answer the above question, we compare characteristics of multiplicity distributions for processes initiated by different partners.

Average multiplicities. Total yields of charged particles in high energy e^+e^-, $p\bar{p}$, pp and central AA collisions become similar if special rescaling has been done. The average charged particle multiplicity in $pp/p\bar{p}$ is similar [41] to that for e^+e^- collisions if the effective energy s_{eff} is inserted in place of s, where $\sqrt{s_{eff}}$ is the $pp/p\bar{p}$ center-of-mass energy minus the energy of the leading particles. In practice, $\sqrt{s_{eff}} = \sqrt{s}/2$ is chosen. This corresponds to the horizontal shift of empty squares to the diamond positions in Fig. 9 borrowed from [44]. Then the diamonds lie very close to the dashed line, which shows QCD predictions for multiplicities in e^+e^- collisions

according to (17). For central nucleus-nucleus collisions the particle yields have been scaled by the number of participating nucleon pairs $N_{part}/2$. Then the energy dependence of mean multiplicities is very similar for all these processes at energies exceeding 10 GeV up to 1 TeV, and even at lower energies for e^+e^- compared with $pp/p\bar{p}$. This is well demonstrated in Fig. 9.

However, the situation changes at higher energies. In Table 2 we show experimentally measured mean multiplicities at Tevatron energies (first row). They are compared with the results of IPPI-model in the second row, where the IPPI predictions at 14 TeV (LHC) and 100 TeV are also shown. According to the above hypothesis, these values should coincide with QCD predictions (17) at twice smaller energy. The latter ones are presented in the third row. The difference between them and experimentally measured values of the first row is demonstrated in the fourth row for Tevatron energies, while at higher energies the difference of QCD and IPPI predictions is shown.

Table 2.

The mean multiplicities at Tevatron and higher energies.

$\sqrt{s}$, GeV	300	546	10^3	$1.8{\cdot}10^3$	$1.4{\cdot}10^4$	10^5
$n_{p\bar{p},exper.}$	25.4	30.5	39.5	45.8	–	–
$n_{p\bar{p},theor.}$	24.1	30.0	39.4	45.7	71.6	97.0
$n_{e^+e^-,theor.}$	25.3	31.8	39.9	49.2	98.2	180
$n_{e^+e^-} - n_{p\bar{p}}$	0.1	1.3	0.4	3.4	26.6	83

It is seen that both experimental and theoretical values of average multiplicity coincide pretty well in $p\bar{p}$ and e^+e^- up to 1 TeV. However, already at Tevatron energy 1.8 TeV the rescaled $p\bar{p}$ multiplicity is lower by 3.4 charged particles. This difference between rescaled predictions of IPPI-model for $p\bar{p}$ and QCD for e^+e^- becomes extremely large at LHC (26.6), and even more so at higher energies.

With these observations, one tends to claim (if at all!) the approximate quantitative similarity of all processes up to 1 TeV and "a universal mechanism of particle production in strongly-interacting systems controlled mainly by the amount of energy available for particle production" [44] only at energies below highest Tevatron values. The situation becomes even worse if we compare other features of multiplicity distributions.

H_q **moments.** First, we have calculated [45] H_q moments for experimental multiplicity distributions in various high energy processes. They are shown in Fig. 10. These moments weakly depend on energy in the energy regions available to present experiments. Their oscillating shape is typical for all processes. However, one notices that amplitudes of H_q oscillations in Fig. 10 differ in various reactions. They are larger for processes with participants possessing more complicated internal structure. For example, amplitudes in e^+e^- are about two orders of magnitude smaller than those in pp. Both QCD applied to e^+e^- [2, 31] and models of $pp/p\bar{p}$ [26] can fit these observations.

There is, however, one definite QCD prediction, which allows to ask a question whether QCD and, e.g., IPPI-model are compatible, in principle. This is the asymptotical behavior of H_q moments in QCD. They should behave [18] as $H_q^{as} = 1/q^2$. One can also determine asymptotics of H_q moments in the IPPI-model and compare both approaches [46]. These values are noticeably larger than QCD predictions of $1/q^2$. Thus, QCD and IPPI-model have different asymptotics. It is an open question whether other asymptotic relations for probabilities of multiparton interactions different from those adopted in IPPI-model can be found which would lead to the same behavior

of H_q moments in $p\bar{p}$ and e^+e^- collisions. Only then one can hope to declare for analogy between these processes.

Fractal properties. The particle density within the phase space in individual events is much more structured and irregular than in the sample averaged distribution. However, even for the latter ones fluctuations depend on the phase space of a sample. The smaller is the phase space the larger are the fluctuations. This can be described by the behavior of normalized factorial moments $F_q = \mathcal{F}_q/\langle n\rangle^q$ as functions of the amount of phase space available. In one-dimensional case of the rapidity distributions within the interval δy, the power-like behavior $F_q(\delta y) \propto (\delta y)^{-\phi(q)}$ for $\delta y \to 0$ and $\phi(q) > 0$ would correspond to intermittent phenomenon well known from turbulence. This also shows that created particles are distributed in the phase space in a fractal manner. The anomalous fractal dimension d_q is connected with the intermittency index $\phi(q)$ by the relation $\phi(q) = (q-1)(d-d_q)$, where d is the ordinary dimension of a sample studied ($d = 1$ for the one-dimensional rapidity plot). It has been calculated in QCD [47, 48, 49] only in the lowest order perturbative approximations. The qualitative features of the behavior of factorial moments as functions of the bin size observed in experiment are well reproduced by QCD.

The anomalous dimensions as functions of the order q derived from experimental data are shown in Fig. 11 for various collisions [28]. They are quite large for e^+e^-, become smaller for hh and even more so for AA collisions. This shows that the more structured are the colliding partners, the stronger smoothed are the density fluctuations in the phase space. In some way, this observation correlates with the enlarged amplitudes of H_q oscillations mentioned above.

In any case, this is another indication that it is premature to claim the similarity of e^+e^- and hadron initiated processes. We have compared just some features of multiplicity distributions. There are many more characteristics of the processes which can be compared but this is out of the scope of the present paper.

7 Conclusions.

We have briefly described the theoretical approaches to collisions of high energy particles. They seem to be quite different for various processes. No direct similarity in multiplicity distributions has been observed. According to experimental data, the energy dependence of average multiplicities in different collisions can be similar in energy region above 10 GeV if some rescaling procedures are used. However, this is just the first moment of multiplicity distributions. To speak about their similarity one should compare other moments. Again, the qualitative features of moment oscillations are somewhat similar but quantitatively they differ. The same can be said about the fractal properties of particle densities within the phase space. No deep reasoning for corresponding rescaling has been promoted. Thus, beside our general belief that QCD Lagrangian is at the origin of all these processes, we can not present any serious arguments in favor of similar schemes applicable to the dynamics of the processes. Moreover, QCD and considered models of hadron interactions predict different asymptotics for some characteristics of e^+e^- and $pp(p\bar{p})$. We have considered here just multiplicity distributions. Other inclusive and exclusive characteristics also seem to be different in these processes.

To conclude, multiplicity distributions in various high energy processes possess some common qualitative features but differ quantitatively. Theoretical approaches to their description have very little in common. Thus, it is premature to claim their common dynamical origin independently of our belief in QCD as a theory of strong interactions.

Acknowledgements.

This work has been supported in part by the RFBR grants 02-02-16779, 04-02-16445-a, NSH-1936.2003.2.

Appendix.

The higher is the rank of the moment, the higher multiplicities contribute to it. Therefore the high rank moments are extremely sensitive to the high multiplicity tail of the distribution. At the same time, the energy-momentum conservation and experimental statistics limitations are important at the tail of the distribution. Therefore, the question about the limits of applicability of the whole approach is quite reasonable.

Let us estimate the range of validity of considering large q values of H_q moments imposed by some cut-offs (see also [35]). It is well known that experimental cut-offs of multiplicity distributions due to the limited statistics of an experiment can influence the behavior of H_q moments. Consequently, they impose some limits on q values allowed to be considered when a comparison is done. Higher rank moments can be evaluated if larger multiplicities have been measured. To estimate the admissible range of q, we use the results obtained in QCD. Characteristic multiplicities that determine the moment of the rank q can be found. By inverting this relation, one can write the asymptotic expression for the characteristic range of q [20]. This provides the bound $q_{max} \approx C n_{max}/\langle n \rangle$ where $C \approx 2.5527$. However, it underestimates the factorial moments. Moreover, the first moment is not properly normalized (it becomes equal to $2/C$ instead of 1). The strongly overestimated values (however, with a correct normalization of the first moment) are obtained if C is replaced by 2. Hence, one can say that the limiting values of q are given by inequalities

$$2n_{max}/\langle n \rangle < q_{max} \leq C n_{max}/\langle n \rangle. \tag{29}$$

The ratio $n_{max}/\langle n \rangle$ measured by E735 collaboration at 1.8 TeV is about 5. Thus, q_{max} should be in the interval between 10 and 13. The approximate constancy of m and proper fits of H_q demonstrated above persist to even higher ranks.

Figure captions.

Fig. 1. A comparison of H_q moments derived from experimental data at 1.8 TeV (squares) with their values calculated with parameter k=4.4 (dash-dotted line) and 3.7 (solid line) [26].

Fig. 2. The q-dependence of m for k=4.4 (squares), 3.7 (circles) and 7.5 (triangles) [26].

Fig. 3. The multiplicity distribution at 1.8 TeV, its fit at $m = 12.94, k = 4.4$ (solid line). The dash-dotted line demonstrates what would happen if NBD is replaced by Poisson distribution [26].

Fig. 4. The decomposition of the fit in Fig. 3 to 1, 2, 3 and 4 parton-parton collisions [26].

Fig. 5. The energy dependence of m (squares) and its linear extrapolation (circles at 14 and 100 TeV) [26].

Fig. 6. The values of k as calculated with w_j satisfying the relation (22) [26].

Fig. 7. The same-charge multiplicity distributions at 14 TeV and 100 TeV obtained by extrapolation of parameters m and k with 5 active pairs at 14 TeV and 6 at 100 TeV (for IPPI-model: solid line - 14 TeV, k=4.4; dash-dotted - 14 TeV, k=8; dashed -

100 TeV, k=4.4; for the modified ladder model: dotted - 14 TeV, k=4.4) [26].

Fig. 8. The behavior of H_q predicted at 14 TeV (k=4.4 -solid line; k=8 - dash-dotted line) [26].

Fig. 9. The energy dependence of average multiplicities for various processes (a) and their ratio to QCD prediction for e^+e^- collisions (b) [44].

Fig. 10. Oscillations of H_q moments for various processes [45].

Fig. 11. Anomalous fractal dimensions for various processes [28].

References

[1] Khoze, V.A., and Ochs, W., *Int. J. Mod. Phys. A*, 1997, vol. 12, p. 2949.

[2] Dremin, I.M., and Gary, J.W., *Phys. Rep.*, 2001, vol. 349, p. 301.

[3] Giovannini, A., *Nuovo Cim. A*, 1972, vol. 10, p. 713; 1973, vol. 15, p. 543.

[4] Landshoff, P.V., and Polkinghorne, J.C., *Phys. Rev. D*, 1978, vol. 18, p. 3344.

[5] Humpert, B., *Phys. Lett. B*, 1983, vol. 131, p. 461.

[6] Goulianos, K., *Phys. Lett. B*, 1987, vol. 193, p. 151.

[7] E735 Collaboration, Alexopoulos, T., et al., *Phys. Lett. B*, 1998, vol. 435, p. 453.

[8] Walker, W.D., *Phys. Rev. D*, 2004, vol. 69, p. 034007.

[9] Capella, A., Sukhatme, U., Tan, C.I., and Tran Thanh Van, J., *Phys. Lett. B*, 1979, vol. 81, p. 68.

[10] Kaidalov, A.B., *Phys. Lett. B*, 1982, vol. 116, p. 459.

[11] Kaidalov, A.B., and Ter-Martirosyan, K.A., *Phys. Lett. B*, 1982, vol. 117, p. 247; *Sov. J. Nucl. Phys.*, 1984, vol. 40, p. 135.

[12] Matinyan, S.G., and Walker, W.D., *Phys. Rev. D*, 1999, vol. 59, p. 034022.

[13] Gaisser, T.K., and Halzen, F., *Phys. Rev. Lett.*, 1985, vol. 54, p. 1754.

[14] Giovannini, A., and Ugoccioni, R., *Phys. Rev. D*, 1999, vol. 59, p. 094020.

[15] Bourelly, C., et al., *Proc. of the VI Blois Workshop on Frontiers in Strong Interactions*, Ed. Tran Thanh Van, J., Editions Frontiers, 1995, p.15.

[16] McLerran, L., *Rev. Mod. Phys.*, 1986, vol. 58, p. 1021.

[17] Shuryak, E., hep-ph/0312227.

[18] Dremin, I.M., *Phys. Lett. B*, 1993, vol. 313, p. 209.

[19] Dokshitzer, Yu.L., Khoze, V.A., Mueller, A.H., and Troyan, S.I., *Basics of perturbative QCD*, Ed. Tran Thanh Van, J., Gif-sur-Yvette, Editions Frontieres, 1991.

[20] Dokshitzer, Yu.L., *Phys. Lett. B*, 1993, vol. 305, p. 295.

[21] Dremin, I.M., and Chernavsky, D.S., *ZhETF*, 1980, vol. 38, p. 229.

[22] Amati, D., Fubini, S., Stanghellini, S., and Tonin, A., *Nuovo Cim.*, 1962, vol 26, p. 896.

[23] Akimov, V.N., Chernavsky, D.S., Dremin, I.M., and Royzen, I.I., *Nucl. Phys. B*, 1969, vol. 14, p. 285.

[24] Dremin, I.M., and Dunaevsky, A.M., *Phys. Rep.*, 1975, vol. 18, p. 159.

[25] Giovannini, A., and Van Hove, L., *Z. Phys. C*, 1986, vol. 30, p. 391.

[26] Dremin, I.M., and Nechitailo, V.A., hep-ph/0402286.

[27] Andersson, B., *The Lund Model*, Cambridge Monogr. Part. Phys. Nucl. Phys. Cosmol., 1997, vol. 7.

[28] De Wolf, E.A., Dremin, I.M., and Kittel, W., *Phys. Rep.*, 1996, vol. 270, p. 1.

[29] Dremin, I.M., and Nechitailo, V.A., *Mod. Phys. Lett. A*, 1994, vol. 9, p. 1471; *JETP Lett.*, 1993, vol. 58, p.881.

[30] Dremin, I.M., and Hwa, R.C., *Phys. Rev. D*, 1994, vol. 49, p. 5805; *Phys. Lett. B*, 1994, vol. 324, p. 477.

[31] Buican, M.A., Förster, C., and Ochs, W., *Eur. Phys. J. C*, 2003, vol. 31, p. 57..

[32] Dremin, I.M., Arena, V., Boca, G., et al., *Phys. Lett. B*, 1994, vol. 336, p. 119.

[33] SLD Collaboration, Abe, K., et al., *Phys. Lett. B*, 1996, vol. 371, p. 149.

[34] L3 Collaboration, Achard, P., et al., *Phys. Lett. B*, 2003, vol. 577, p. 109.

[35] Dremin, I.M., and Nechitailo, V.A., *Eur. Phys. J. direct C*, 2003, vol. 5, p. 04.

[36] Giovannini, A., and Ugoccioni, R., *Phys. Rev. D*, 2003, vol. 68, p. 034009.

[37] Sarkisyan, E.K.G., *Phys. Lett. B*, 2000, vol. 477, p. 1.

[38] UA5 Collaboration, Arnison, G., et al., *Phys. Lett. B*, 1982, vol. 118, p. 167.

[39] E735 Collaboration, Turkot, F., et al., *Nucl. Phys. A*, 1991, vol. 525, p. 165.

[40] Hegyi, S., *Phys. Lett. B*, 1996, vol. 387, p. 642; 1998, vol. 417, p. 186.

[41] Basile, M., et al., *Phys. Lett. B*, 1980, vol. 92, p. 367; 1980, vol. 95, p. 311.

[42] Bertini, M., Lönnblad, L., and Sjöstrand, T., *Comput. Phys. Commun.*, 2001, vol. 134, p. 365; see also http://www.thep.lu.se/˜torbjorn/Pythia.html.

[43] HERWIG 6.5, Corcella, G., Knowles, I.G., Marchesini, G., Moretti, S., Odagiri, K., Richardson, P., Seymour, M.H., and Webber, B.R., *JHEP*, 2001, vol. 0101, p. 010; see also http://hepwww.rl.ac.uk/theory/seymour/herwig/.

[44] PHOBOS Collaboration, Back, B.B., et al., hep-ex/0301017.

[45] Dremin, I.M., Nechitailo, V.A., Biyajima, M., and Suzuki, N., *Phys. Lett. B*, 1997, vol. 403, p. 149.

[46] Dremin, I.M., hep-ph/0404092; *Proc. of XXXIX Rencontres de Moriond*, Ed. Tran Thanh Van, J., 2004.

[47] Ochs, W., and Wosiek, J., *Phys. Lett. B*, 1992, vol. 289, p. 159; 1993, vol. 304, p. 144.

[48] Dokshitzer, Yu.L., and Dremin, I.M., *Nucl. Phys. B*, 1993, vol. 402, p. 139.

[49] Brax, Ph., Meunier, J.L., and Peschanski, R., *Z. Phys. C*, 1994, vol. 62, p. 649.

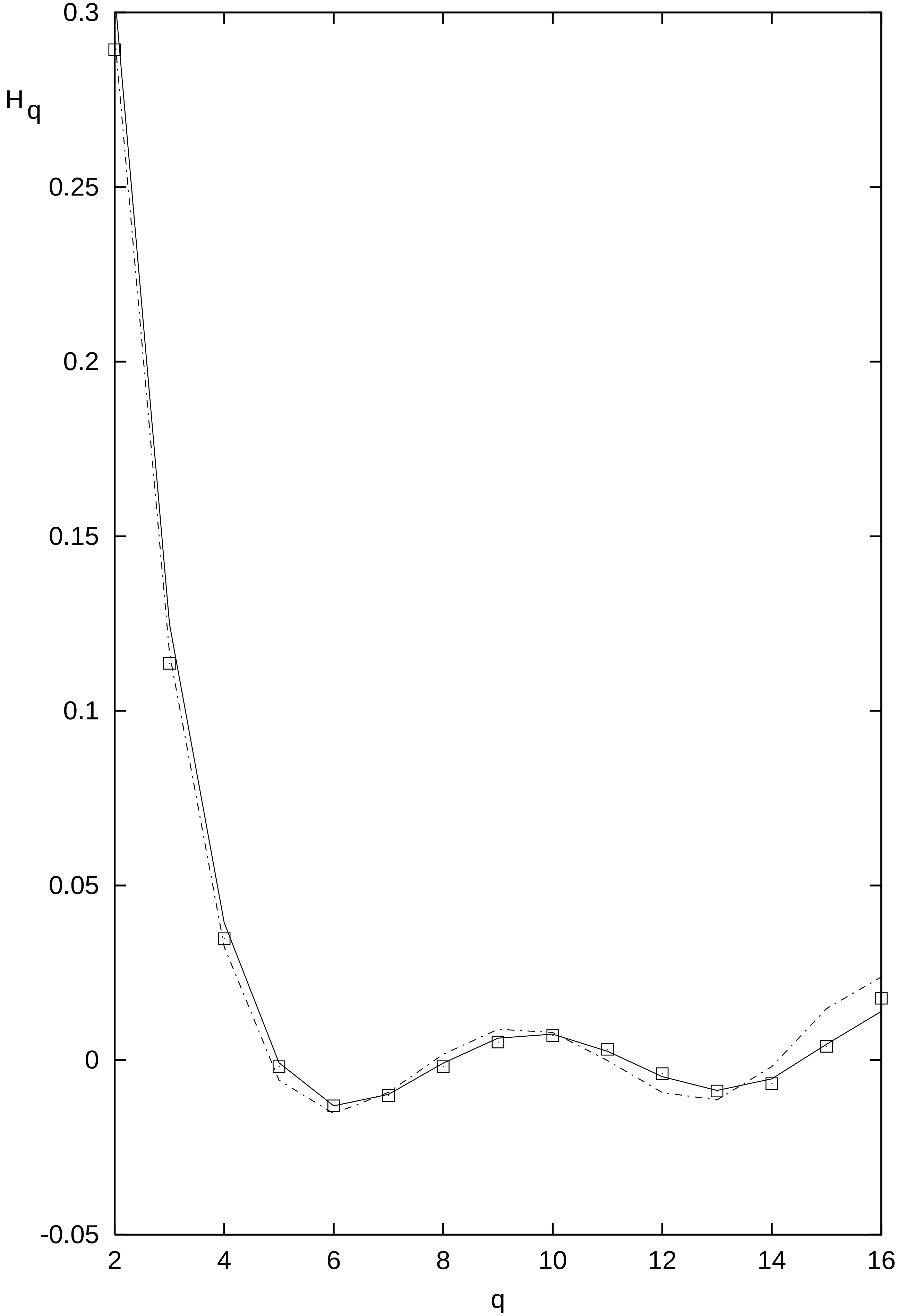
0.3
0.25
0.2
0.15
0.1
0.05
0
-0.05
H_q
2
4
6
8
10
12
14
16
q

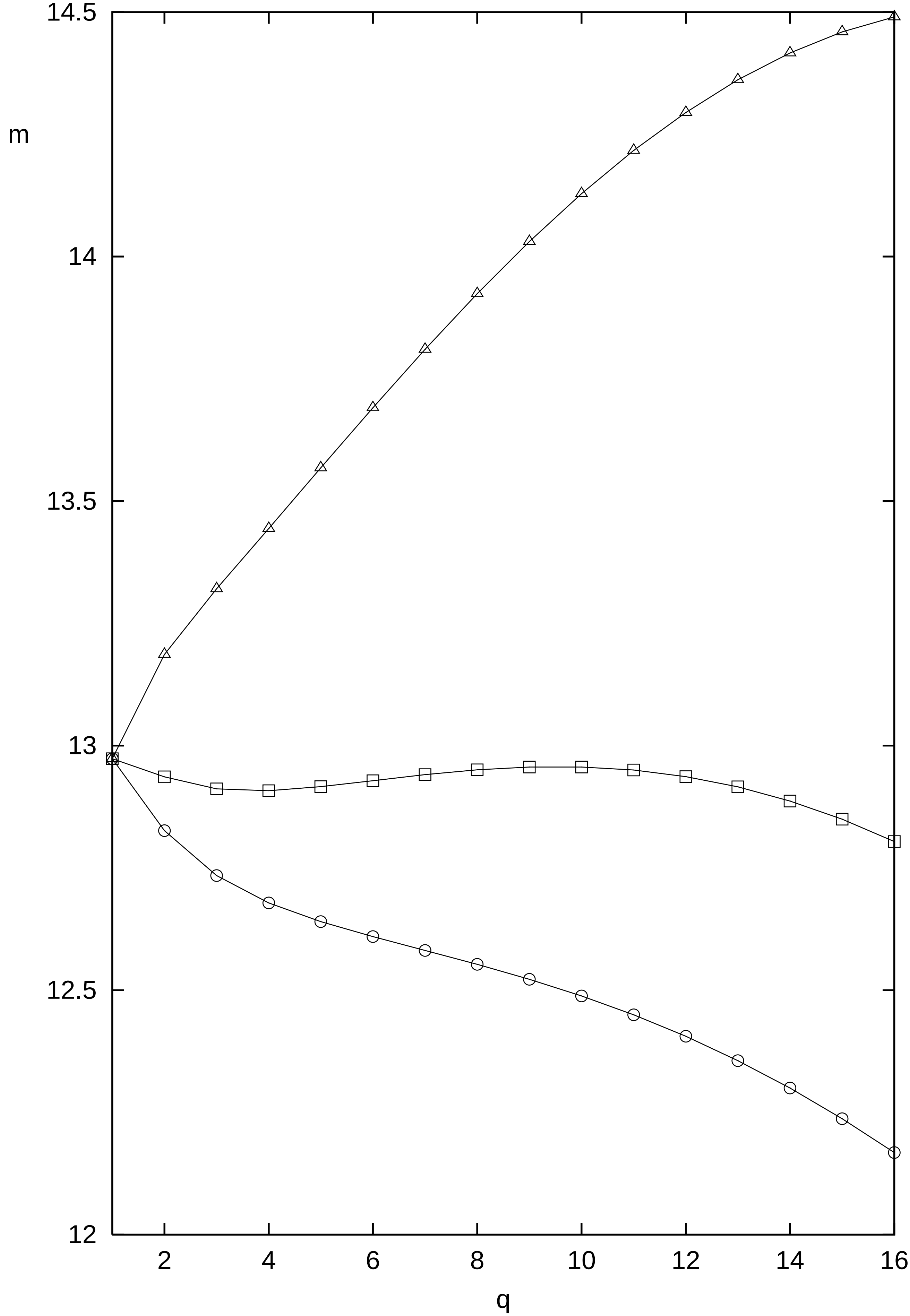

m
14.5
14
13.5
13
12.5
12
2
4
6
8
10
12
14
16
q

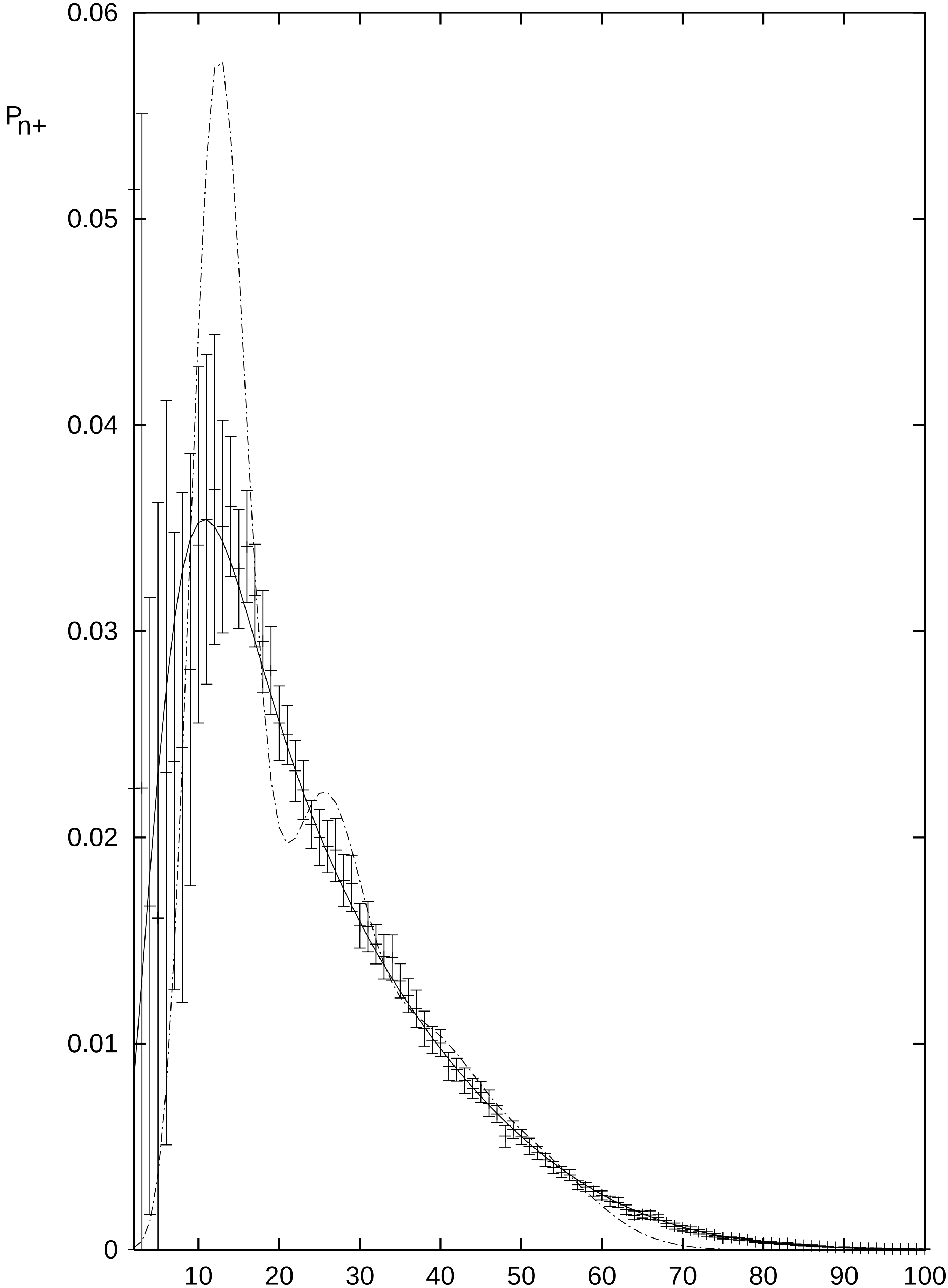

0.06
0.05
0.04
0.03
0.02
0.01
0
P_{n+}
10
20
30
40
50
60
70
80
90
100
n+

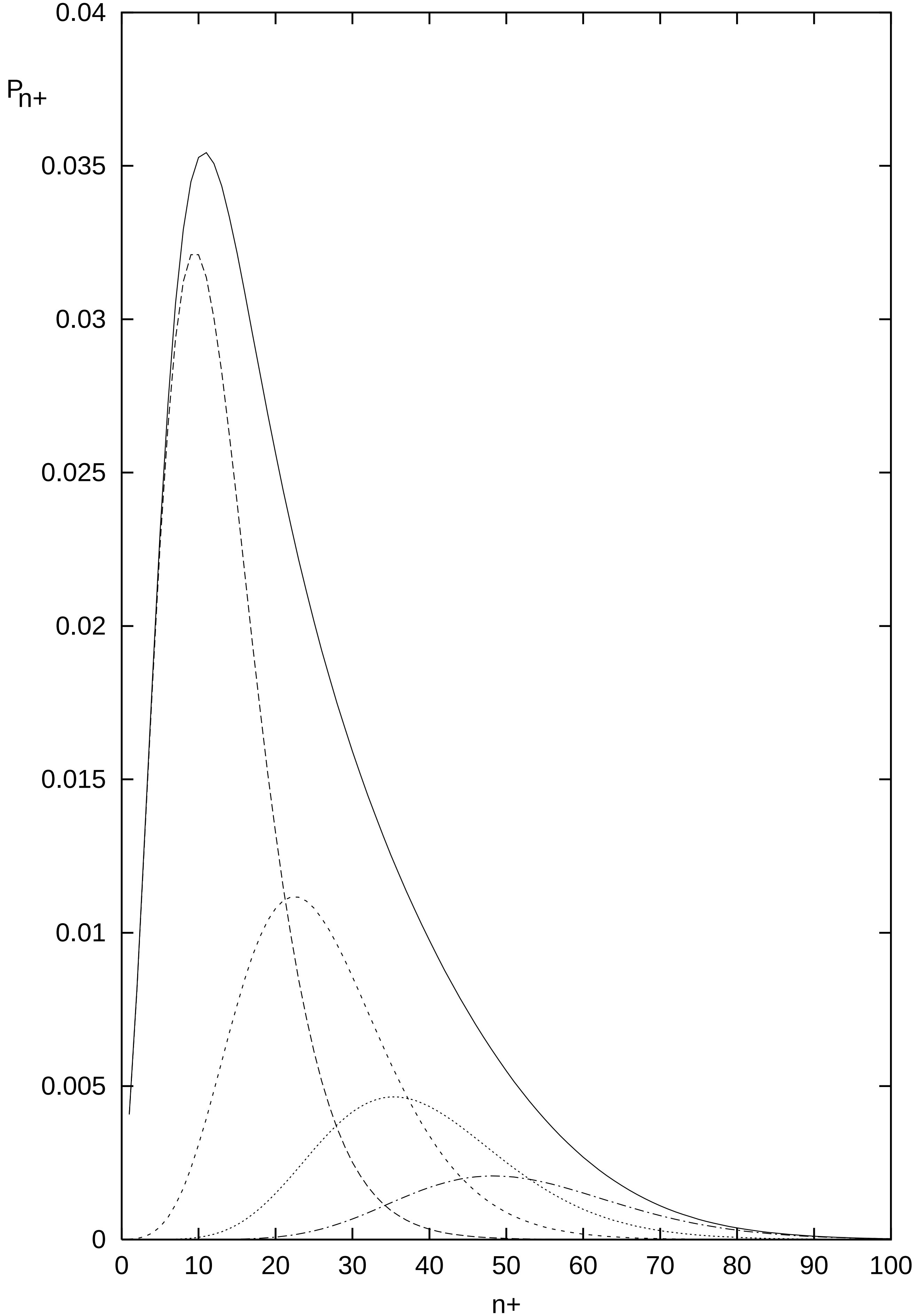

0.04
0.035
0.03
0.025
0.02
0.015
0.01
0.005
0
P n+
0
10
20
30
40
50
60
70
80
90
100
n+

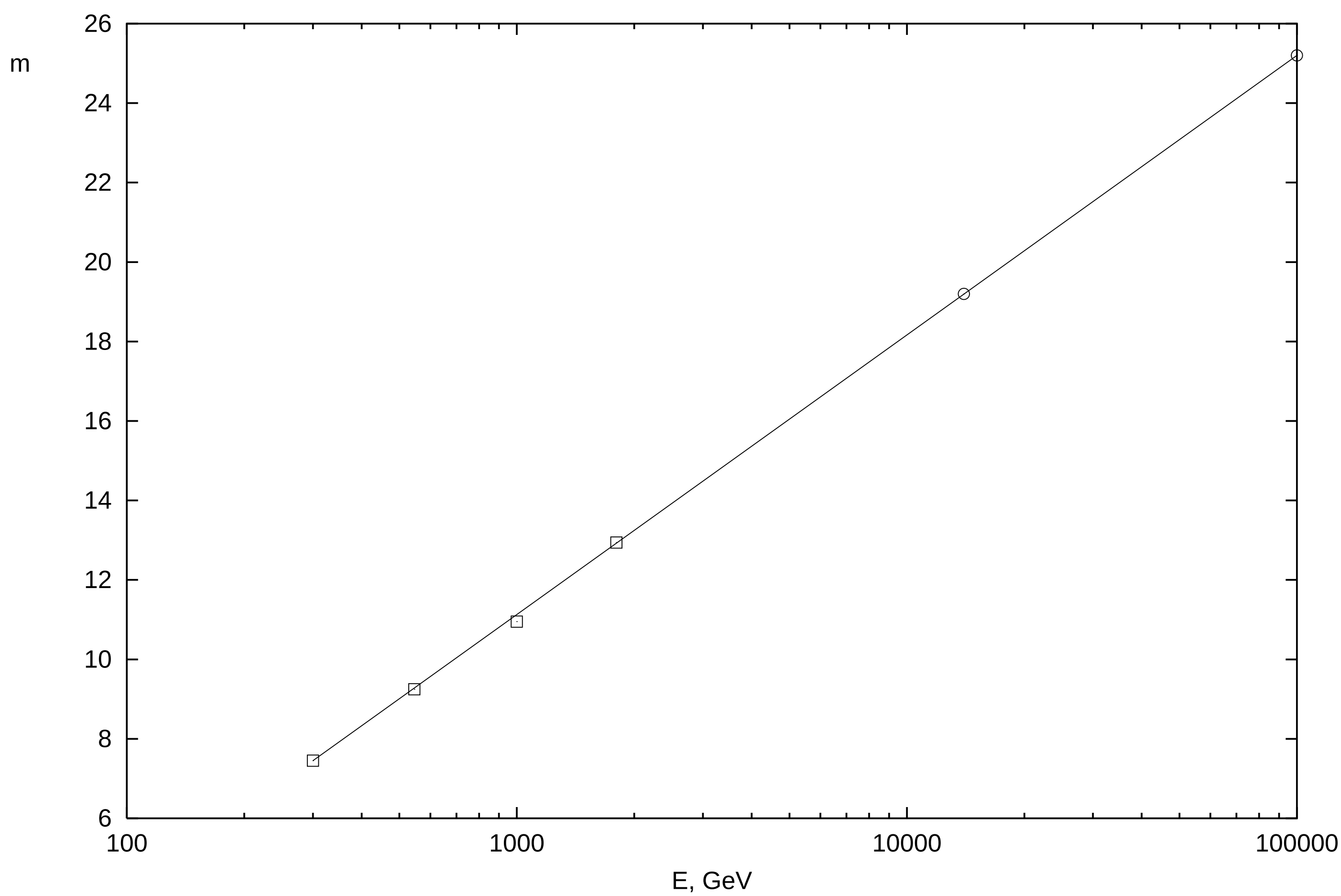
m
26
24
22
20
18
16
14
12
10
8
6
100
1000
10000
100000
E, GeV

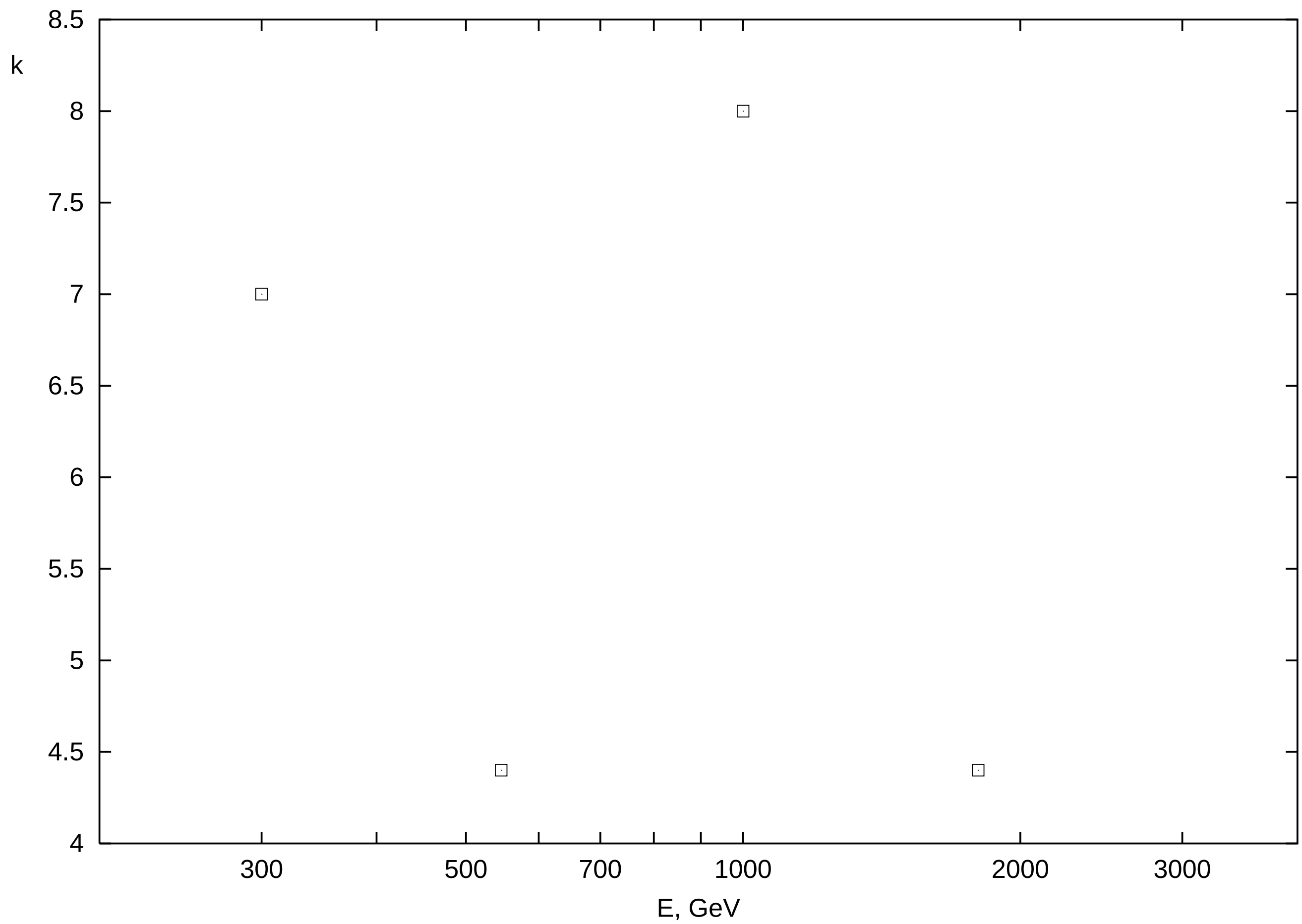
k
8.5
8
7.5
7
6.5
6
5.5
5
4.5
4
300
500
700
1000
2000
3000
E, GeV

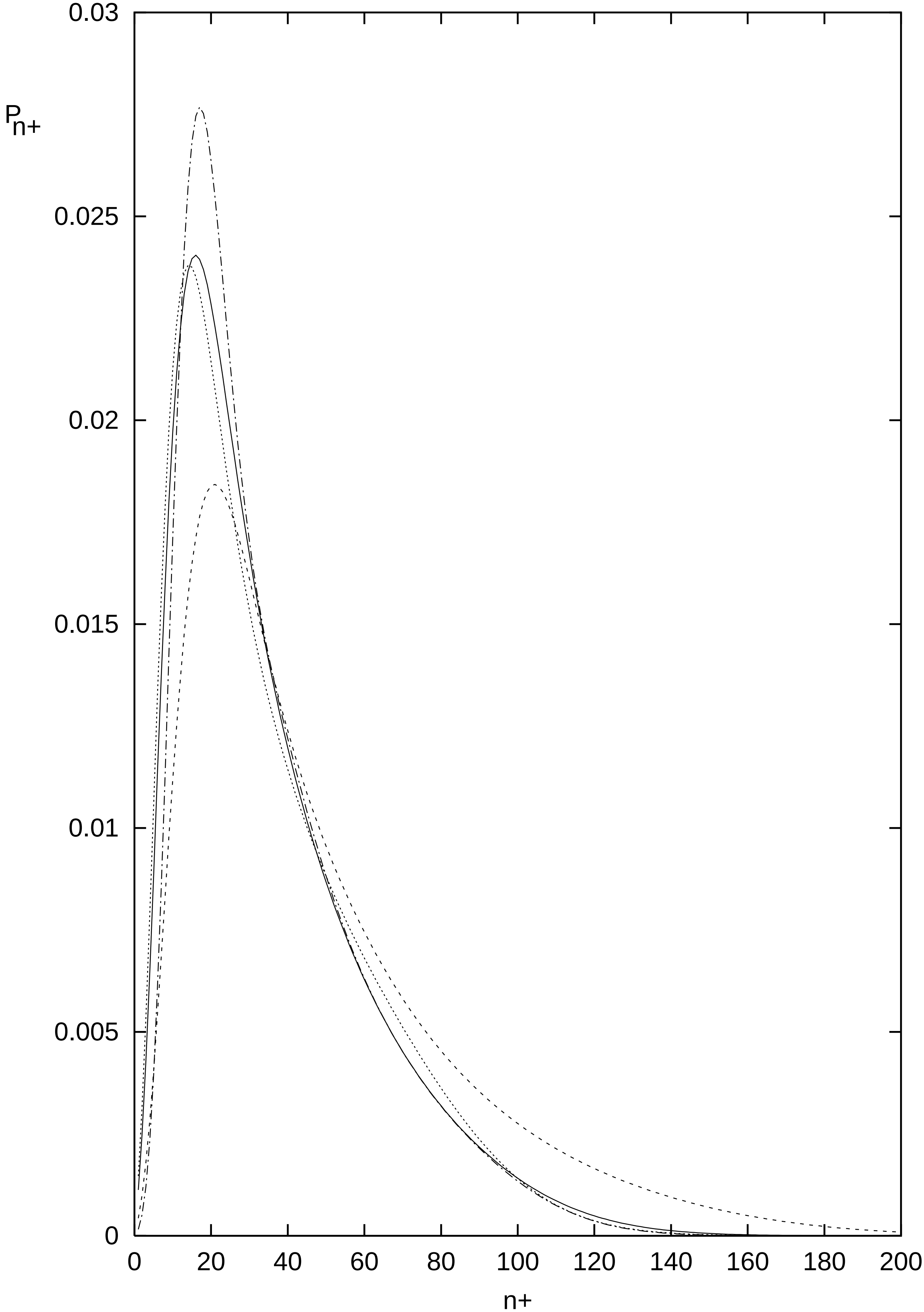

0.03
0.025
0.02
0.015
0.01
0.005
0
P n+
0
20
40
60
80
100
120
140
160
180
200
n+

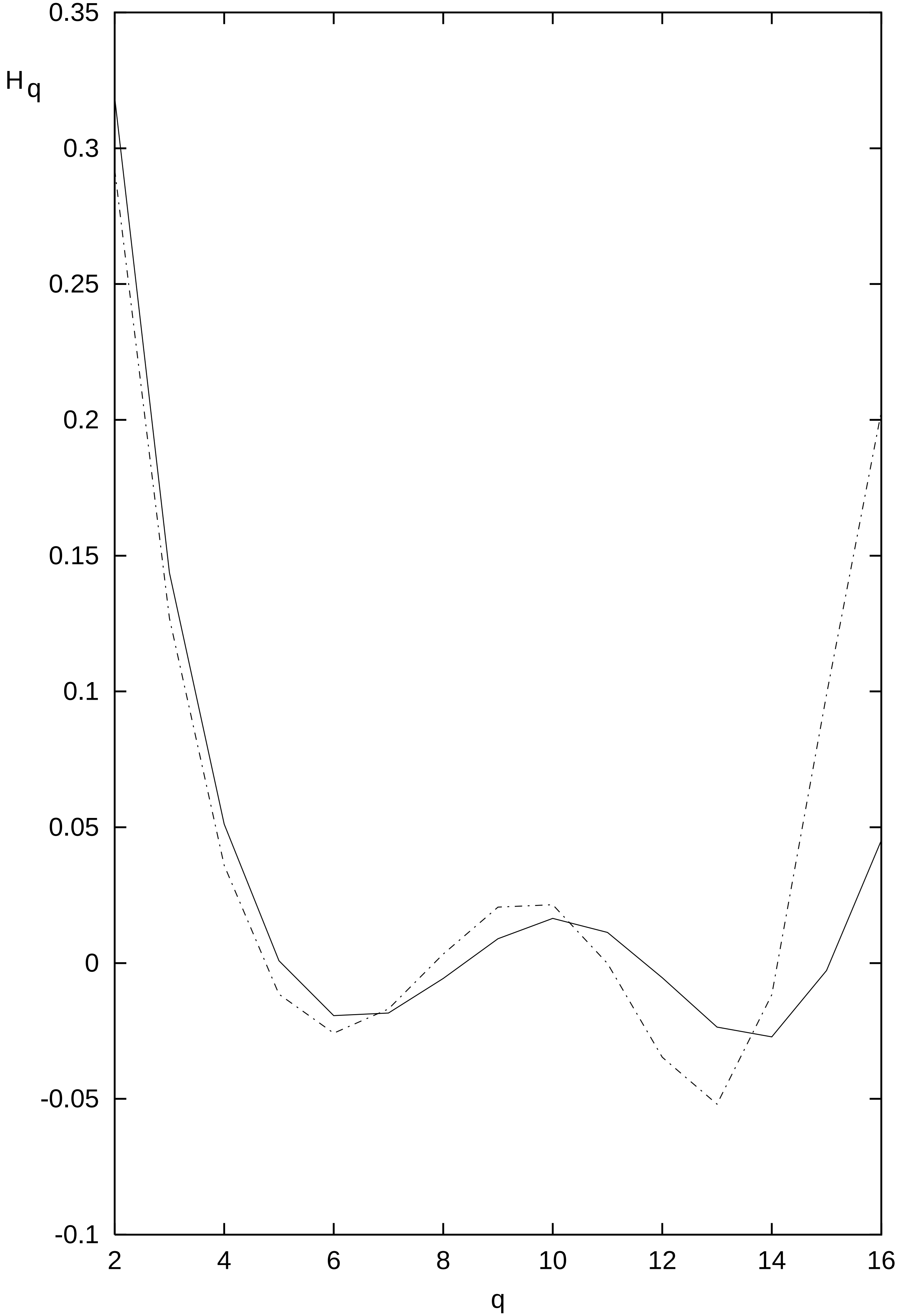

H q
0.35
0.3
0.25
0.2
0.15
0.1
0.05
0
-0.05
-0.1
2
4
6
8
10
12
14
16
q

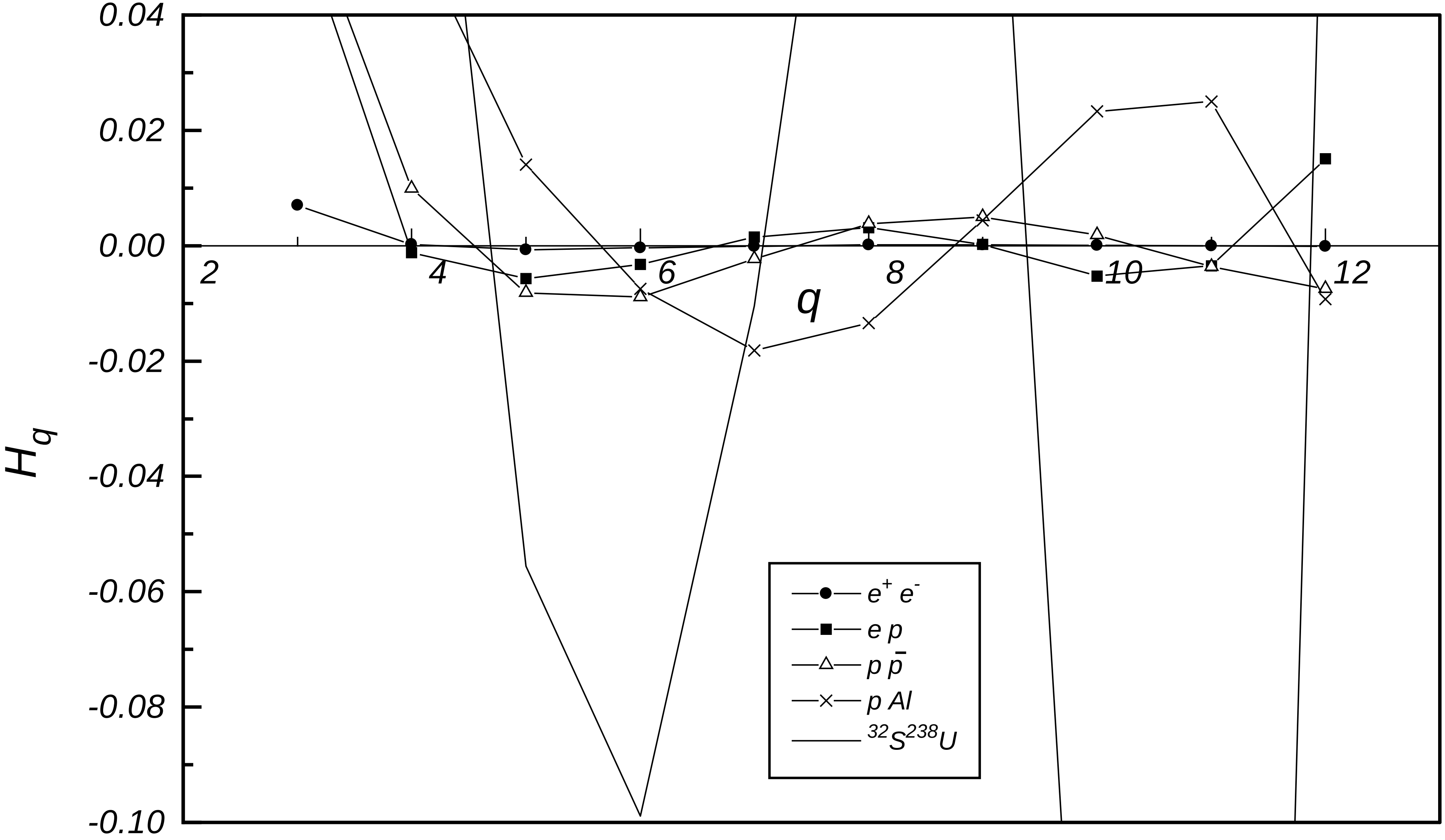

0.04
0.02
0.00
-0.02
-0.04
-0.06
-0.08
-0.10
2
4
6
8
10
12
q
H_q
e+ e-
e p
p p̄
p Al
32S238U